Noninvasive Estimation of Tissue Temperature Via High-Resolution Spectral Analysis Techniques

Ali Nasiri Amini*, *Student Member, IEEE*, Emad S. Ebbini, *Member, IEEE*, and Tryphon T. Georgiou, *Fellow, IEEE*

***Abstract*—We address the noninvasive temperature estimation from pulse-echo radio frequency signals from standard diagnostic ultrasound imaging equipment. In particular, we investigate the use of a high-resolution spectral estimation method for tracking frequency shifts at two or more harmonic frequencies associated with temperature change. The new approach, employing generalized second-order statistics, is shown to produce superior frequency shift estimates when compared to conventional high-resolution spectral estimation methods Seip and Ebbini (1995). Furthermore, temperature estimates from the new algorithm are compared with results from the more commonly used echo shift method described in Simon *et al.* (1998).**

***Index Terms*—Diagnostic ultrasound, maximum entropy, spectral analysis, state-covariance, super-resolution.**

I. Introduction

NONINVASIVE temperature estimation continues to attract attention as a means of monitoring and guidance for minimally invasive thermo-therapy. Currently, magnetic resonance imaging (MRI) and ultrasound have both been proven to have the temperature sensitivity and spatial resolution necessary to provide noninvasive temperature feedback. The main limitation for MRI is the cost and the potential complication of the heating protocol as the heating equipment must be MR compatible. Ultrasound is relatively less expensive, portable, and can be used in conjunction with almost any heating protocol without adding any significant constraints. Therefore, noninvasive temperature estimation based on ultrasound echo data continues to be an important problem in the area of image-guided minimally invasive thermal therapy.

The ultrasound tissue characterization literature makes extensive use of a discrete scatterer model assuming that the echo signal is a superposition of echoes from a semi-regular lattice of point scatterers within the resolution cell of the imaging system (see [3]). This model assumes that the echo signal reflects the backscatter from specular, regular, and diffuse scatterers. In cases when regular scatterers exist within the resolution cell, the power spectrum exhibits peaks at harmonic frequencies related to the mean scatterer spacing (MSS). In [1], it was shown that the local temperature change produces proportional shifts in these harmonic frequencies. The proportionality factor is related to the change in speed of the sound and the local expansion. Thus, a quantitative estimation of tissue temperature becomes feasible by tracking the frequency shifts if the harmonics can be reliably estimated from the spectra of the echo signals.

In [1], the autoregressive (AR) spectral estimation was applied to estimate the frequency shifts. While this approach validated the MSS model and its use in temperature estimation, the bias and variance in the frequency shift estimates made it difficult to develop a robust algorithm for temperature estimation. It was suggested that three or more peaks in the AR spectrum be "fit" to a harmonic model to improve the consistency of the results.

Recent advances in nonlinear spectral analysis empowered us to design algorithm with higher resolution [4], [5]. These algorithms are constructed based on a new formalism for spectral estimation where generalized second-order statistics are derived from data to estimate power spectral density. Generalized second-order statistics are natural generalization of covariances which are the basis for the classical techniques like AR. The new framework enables us to control the resolution in different frequency bands. We use this property to design an adaptive algorithm to track very small frequency shifts. Interestingly, the experimental results validate the theoretical prediction of existing harmonic frequencies.

It is important to note that there are a number of different approaches to temperature estimation based on backscatter ultrasound. One of the more computationally attractive approaches is described in [2] where temperature change in the tissue has been related to the axial derivative of the echo shift from a scatterer (or a collection of scatterers) at a given location. Not surprisingly, the proportionality is also related to the local change in speed of sound and thermal expansion. However, the echo shift method does not depend on the existence of regular scatterers within the analysis window. The main limitation of this method is the phenomenon described in [2] as thermal lens effect due to the ultrasonic beam distortion as it propagates through the heated region. In addition, this method is less quantitative as it is not related to a specific tissue structure with known behavior in response to temperature change. Nonetheless, this method is extremely attractive as it produces two-dimensional temperature images that can be used to map the extent of the heated region, with obvious implications for image guidance.

Manuscript received December 1, 2003; revised May 31, 2004. This work was supported in part by the National Science Foundation (NSF) and in part by the Air Force Office of Scientific Research (AFOSR). *Asterisk indicates corresponding author.*

*A. Nasiri Amini is with the Department of Electrical and Computer Engineering, University of Minnesota, Minneapolis, MN 55455 USA (e-mail: nasiri@ece.umn.edu).

E. S. Ebbini is with the Department of Electrical and Computer Engineering, University of Minnesota, Minneapolis, MN 55455 USA (e-mail: emad@ece.umn.edu).

T. T. Georgiou is with the Department of Electrical and Computer Engineering, University of Minnesota, Minneapolis, MN 55455 USA (e-mail: tryphon@ece.umn.edu).

Digital Object Identifier 10.1109/TBME.2004.840189

The organization of the paper is as follows. In Section II, the essence of estimating temperature from ultrasound echo is discussed. Section III briefly explains the new high-resolution spectral analysis framework. In Section IV, we use new framework to design an algorithm to estimate frequency shifts and apply it on experimental data. The results of Section IV are discussed in Section V, and concluding remarks are given in Section VI.

II. Temperature Estimation

The temperature change estimation method in this paper is based on the thermal dependence of the ultrasound echo that accounts for two different physical phenomena: local change in speed of sound and thermal expansion of the propagating medium due to changes in temperature. The speed of sound c is a function of temperature. In most tissue media around body temperature, c increases with temperature in the range (see [7, pp. 106–110]). In fatty tissues, c decreases with increasing temperature [1]. For a tissue region with quasiregular scatterer lattice, the average distance between scatterers is known as mean scatterer spacing, d. Thermal expansion and contraction of the medium due to changes in temperature affects the mean scatterer spacing. Despite the complexity of the spectrum of the echo signal, the presence of a quasiregular lattice of scatters produces harmonically related peaks with fundamental frequency $f_1 = (c/2d)$. This can be explained through the discrete tissue scattering model which is widely accepted in the field of tissue characterization with diagnostic ultrasound (cf. [3] and [8]). This model is based on the assumption that the backscattered A-line signal, $y(t)$, consists of a superposition of scaled and shifted versions of the spatially varying impulse response $p_i(\cdot)$ of the diagnostic transducer and the medium [9]. In particular

$$y(t) = \sum_{i=1}^{N_s} A_i p_i(t - \tau_i) \tag{1}$$

where N_s represents the number of scatterers within the processing window, t represents time, and A_i is the magnitude of the reflection from ith scatterer along the transducer imaging axis. The term τ_i denotes the two-way travel time of the diagnostic pulse from the face of the transducer to the ith scattering center and back to the transducer.

Assuming the above model, it can be shown that the power spectral density (PSD) of the backscattered signal $y(t)$ has resonances related harmonically (see [1]). More precisely whenever scatterers are uniformly spaced the PSD of $y(t)$, $S_y(f)$, has peaks at

$$f_k(T) = \frac{kc(T)}{2d(T)} \quad \text{where } k = 1, \ldots, \infty. \tag{2}$$

When the distance between scatterers is not uniform, but has some level of regularity, the local peaks in the PSD will be determined by the average distance between scattering centers d. The larger the variance in the scatterer spacing distribution, the wider are the resonant peaks in the PSD.

Temperature change affects local value of the speed of sound and mean scatterer spacing of the medium. Thus, f_k is a function of the local temperature of the medium. The change in f_k, Δf_k, due to the temperature change can be found by differentiating (2) with respect to T and is given by

$$\frac{\partial f_k(T)}{\partial T} = \frac{k}{2}\left[\frac{\partial c(T)}{\partial T}\frac{1}{d(T)} - \frac{\partial d(T)}{\partial T}\frac{c(T)}{d^2(T)}\right].$$

Using forward differencing approximation of $\partial f_k(T)/\partial T$ at a given temperature, T_0, one can get the following:

$$\frac{\Delta f_k(T)}{\Delta T} \approx \frac{k}{2}\left[\frac{\partial c(T)}{\partial T}\left.\frac{1}{d(T)}\right|_{T=T_0} - \left.\frac{\partial d(T)}{\partial T}\frac{c(T)}{d^2(T)}\right|_{T=T_0}\right]. \tag{3}$$

Strictly speaking, T_0 is function of space and time. However, in practice, the proportionality coefficient in (3) is constant for a range of ΔT up to 15 °C from normal body temperature. Therefore, it is reasonable to assume T_0 constant throughout the temperature range of interest. For values of ΔT higher the 20 °C, the whole approach based on echo ultrasound is likely to fail. Under such conditions, one may want to account for T_0 as a function of time and space. This is beyond the scope of this paper.

A reasonable approximation of mean scatterer spacing as a function of temperature is given by

$$d = d_0(1 + \alpha\Delta T), \tag{4}$$

where α is the linear coefficient of thermal expansion of the medium and d_0 is the mean scatterer spacing at the baseline temperature T_0. Let c_0 be the speed of sound in the medium at the baseline temperature of T_0. Using (4) in (3), we obtain

$$\Delta f_k(T) \approx k\Lambda\Delta T \tag{5}$$

where Λ is defined as

$$\Lambda := \frac{1}{2d_0}\left[\left.\frac{\partial c(T)}{\partial T}\right|_{T=T_0} - \alpha c_0\right]. \tag{6}$$

Equation (5) explains the approximately linear relation between Δf_k and ΔT.[1] Note that the constant Λ combines two different effects, the change in the speed of sound and the change in mean scatterer spacing (cf. [1]).

There is an alternative approach of using ultrasound to estimate temperature change. As it was explained the temperature change causes two physical phenomena: local change in speed of sound and thermal expansion. The former produces an apparent shift in scatterer location, and the latter leads to a physical shift. Along an A-line, however, the two effects amount to echo time-shifts. Let z, and δt denote the axial depth and time-shift, respectively. It has been shown in [2] that

$$\Delta T(z) = c_0 \cdot k_m \cdot \frac{\partial}{\partial z}(\delta t(z))$$

where k_m is a medium (material) dependent parameter. For a homogeneous medium this parameter can be experimentally determined. Therefore, temperature-change estimates can be obtained by first tracking the cumulative echo time-shift at each location, and then differentiating it along the axial direction z and filtering along both axial and lateral x directions. This method

[1]Note that Λ is a constant that depends on the medium structure and on temperature. Therefore, this constant must be appropriately updated as temperature changes are computed.

was explained and discussed in detail in [2]. Section V the performance of this method (time-shift) is compared to our method which is based on frequency shift estimation.

III. High Resolution Spectral Analysis

Classical high resolution spectral estimation techniques typically rely on estimates of covariance lags

$$R_n := \{r_0, r_1, r_2, \ldots, r_n\}$$

where $r_k := \mathrm{E}\{y(t)y(t-k)^*\}$, and "$*$" denotes complex conjugate. Here, $n \ll N$, where N is the number of data points. Given R_n, in general, there exists a family of power spectra consistent with R_n. The variety in high resolution algorithms stems from the different criteria that they apply to pick one spectrum from this family. For instance, AR and MUSIC postulate some models for the random signal and choose the spectrum that satisfies the presumed model. On the other hand, the criterion could be maximization of an objective function like maximum entropy (ME) method where the spectrum with the largest entropy is sought [10].

Recently a new framework has been developed, which uses the generalized second-order statistics instead of covariance lags. The mathematical theory for this approach was developed in [5], [11], and [12], where its superior statistical properties have been demonstrated in [13]. Next, we review the new formalism and apply it to design algorithms for frequency shift estimation.

Consider the (discrete-time) state equations

$$x(k) = Ax(k-1) + By(k), \quad \text{for k} \in \mathbb{Z}. \tag{7}$$

Throughout, we assume that $x \in \mathbb{C}^{n\times 1}, A \in \mathbb{C}^{n\times n}$ and $B \in \mathbb{C}^{n\times 1}$. Also (A, B) is a controllable pair and the eigenvalues of A have modulus less than one.

State-space equation (7) represents a filter which has one dimensional input and n dimensional output (i.e., vector $x(k)$). We refer to this filter as input-to-state (IS) filter. The transfer function of IS filter is given by

$$G(\mathrm{z}) = (I - \mathrm{z}^{-1}A)^{-1}B. \tag{8}$$

Assume that the above filter is driven by a zero-mean stationary stochastic process $y(k)$ for long time, in other words we have reached steady state. Then the covariance of the output $x(k)$ is defined by

$$P := \mathrm{E}\{x(k)x(k)^*\}$$

and "$*$" denotes complex conjugate transpose. The matrix P, which is referred by state covariance, is a generalization of second-order statistics. In practice, P is not available and should be estimated from the data. To this end, the IS filter is driven by the samples of the underlying process $\{y(0), y(1), \ldots, y(N-1)\}$ and generates $\{x(0), x(1), \ldots, x(N-1)\}$. Then P can be estimated by

$$\hat{P} = \frac{1}{N}\sum_{k=0}^{N-1} x(k)x(k)^*.$$

Similar to classical framework, there is a set of consistent spectra corresponding to state covariance. In [11], a linear fraction parameterization of spectra which are consistent with a P is derived. It is shown that the ME estimator consistent with P is given by

$$S_{\mathrm{ME}}(e^{j\omega}) = \frac{B^*P^{-1}B}{G(e^{j\omega})^*P^{-1}BB^*P^{-1}G(e^{j\omega})}. \tag{9}$$

It should be noted that the new framework encompasses the classical framework. It can be seen by choosing (A, B) as

$$A = \begin{bmatrix} 0 & 0 & \cdots & 0 \\ 1 & 0 & \cdots & 0 \\ 0 & 1 & \cdots & 0 \\ \vdots & & & \\ 0 & \cdots & 1 & 0 \end{bmatrix}, \quad B = \begin{bmatrix} 1 \\ 0 \\ \vdots \\ 0 \end{bmatrix}. \tag{10}$$

In this case, P is given by

$$P = \begin{bmatrix} r_0 & r_1^* & \cdots & r_{n-1}^* \\ r_1 & r_0^* & \ddots & r_{n-2}^* \\ \vdots & \ddots & \ddots & \\ r_{n-1} & r_{n-2} & \cdots & r_0 \end{bmatrix}$$

which is exactly the Toeplitz covariance matrix. Thus, the classical approach is one example of the new framework where (A, B) are chosen as (10).

The key observation to improve resolution is that *the variance of the frequency estimator is a function of* (A, B). In fact, there is a tradeoff between variability of frequency estimates and resolution. The design factor which affects resolution is the frequency response of the IS filter. Using an *IS filter with a bandpass characteristic increases the resolution in the passband* at the expense of resolution elsewhere. This stems from the fact that the state covariance is function of IS filter frequency response. In particular, we have

$$P = \int_{-\pi}^{\pi} G(e^{j\omega})G^*(e^{j\omega})S_y(\omega)\, d\omega.$$

The other factor which adversely affects variance of estimates is time constant of the IS filter [13].

Exploring the structure of the IS filter reveals that the shape of its frequency response is determined by the eigenvalues of the A. Note that IS filter is a single input/multi output filter, thus, to quantify its frequency response we use the 2-norm of the output vector. In particular, if $\{\lambda_i = a_i e^{j\theta_i}\}_{i=1}^n$ denotes the set of the eigenvalues of A, then the frequency response of (8) is given by

$$\|G(e^{j\omega})\|^2 = \sum_{i=1}^{n} \frac{1 - a_i^2}{(1 + a_i^2 - 2a_i\cos(\omega - \theta_i))}. \tag{11}$$

It is evident that each summand is a bandpass filter with θ_i as the center frequency. The other design parameters which determine the Q-factor of the filter are a_i's. The closer a_i to one, the filter is more selective. However choosing a_i close to one makes the time constant large unduly and adversely affects the quality of the estimates (see [14]).

The conclusion is that *the resolution of spectral estimator can be enhanced in a frequency band by choosing the eigenvalues of A reasonably close to that band.* Also from experience it appears that the case when A and B are normalized such that $AA^* + BB^* = I$ is more well-behaved numerically.

In this paper, we choose eigenvalues of A at complex conjugates to address the symmetry of the spectrum of the RF-echo

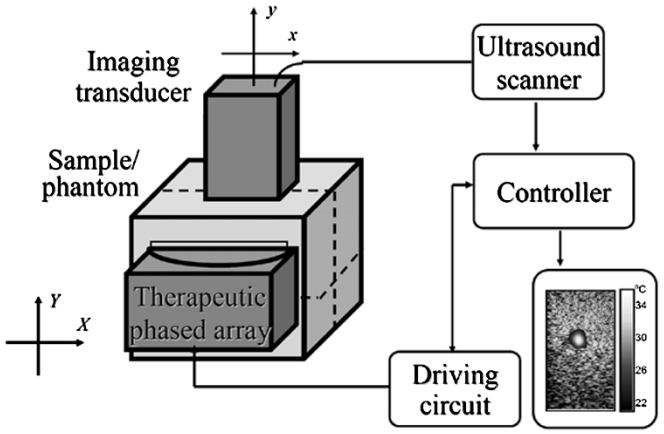

Fig. 1. Diagram of the experimental setup depicting the dual ultrasound system.

data.[2] In particular, we put half of the eigenvalues $(n/2)$ at $ae^{j\theta}$ and the other half at $ae^{-j\theta}$ to enhance the resolution in frequency band around θ and $-\theta$. Thus, the IS filter

$$G_{a,\theta,n}(\mathrm{z}) = (I - \mathrm{z}^{-1}A)^{-1}B \tag{12}$$

is fully characterized by n, a, and θ.

The frequency shift estimation algorithm starts by estimating the spectrum by $a = 0$ which corresponds to a flat IS filter. Then the rough estimates of peaks incorporates in IS filter design by placing multiple eigenvalues close to them. This increases the resolution and enables us to accurately track the peak in time. Note that the order of the IS filter, n, should be chosen based on the length of the data to guarantee the accuracy of the estimated state-covariance. As a rule of thumb we use $n \approx 0.2 \times N$. The mathematical basis for such rules has been developed in [15]. In the Section IV, we apply this technique to estimate the temperature change from the experimental data.

IV. Experiments and Results

In order to illustrate the capabilities of the method presented in this paper, experiments have been conducted in which a medium is heated using the therapeutic transducer while diagnostic RF-echo is collected using the combined imaging/therapy ultrasound system shown in Fig. 1. The setup is similar to that described in [2]. We have collected data using linear array probes on ATL Ultramark 9 (3.5–5 MHz with sampling at 20 MHz) and Esaote MPX (5–9 MHz with sampling at 33 MHz) scanners. In addition, two different phantoms were used. The ATL data was acquired using the phantom described in [2], which consisted of a parallelepiped sample $85 \times 70 \times 48$ mm^3 of rubber material (M-F Manufacturing Co., Fort Worth, TX). Microspheres with diameters 75–150 μm (Amberlite IR-120plus, Sigma Chemical Co., St. Louis, MO) in a concentration of 0.6% by volume acted as ultrasound scatterers. The Esaote data was acquired using a phantom prepared according to the procedure described in [16] and [17]. The phantom was prepared by using 13 g gelatin, 18 ml N-propanol, 18.75 g graphite, and 52 ml glutaraldehyde in 230 ml water. This phantom provides a more realistic approximation of tissue properties with special emphasis on elastic properties. We mention here that the ATL data was acquired while the second author was at the University of Michigan. The results reported in this paper are based on this same ATL data to help the reader compare the results shown in this paper with our previous results shown in [2]. The Esaote data is actually of higher quality than the ATL data, but produced similar results to the ATL data. Therefore, we decided not to include these results in this paper to avoid repetition.

[2]The RF-echo data is real, thus, the spectrum is symmetric.

TABLE I
Parameter Values Used for the Temperature Estimation

Parameter	Value	Units
RF-data sampling frequency	20	MHz
lateral sampling frequency	3.4	mm^{-1}
frame rate of data collection	1	frame/s
axial window size for spectral analysis	3.3	mm
6dB bandwidth of the axial filter	0.14	mm^{-1}
6dB bandwidth of the lateral smoothing filter	0.17	mm^{-1}
length of the axial smoothing filter	12.3	mm
length of the lateral smoothing filter	6.2	mm

Examining (3), one can see that the frequency shift in the kth harmonic is proportional to k. This provide us with a means for establishing the consistency of the temperature measurement. Specifically, the relative frequency shifts at the true harmonics are equal, i.e.,

$$\frac{f_1(t)}{f_1(0)} = \frac{f_2(t)}{f_2(0)} = \cdots.$$

Therefore, different harmonics have the same patterns of the frequency shifts. In practice, only those harmonics within the transducer bandwidth and are not masked by other scattering phenomena are potentially detectable.

A. Algorithm

The new algorithms starts by finding a rough estimates for the resonant frequencies. To this end we use IS filter (12) with $a = 0$ (i.e., nonselective) to estimate PSD peaks. Then an appropriate set of IS filters is formed to track different harmonics. Note that these primary estimates are exactly the achievable estimates in classical approaches like AR. In particular, θ in (12) is chosen as these rough estimates. Designing parameter, a, allows us to control the resolution. However the a should not be too close to 1.0 to prevent the long transient time of the IS filter.

B. Phantom Heating Experiment

The first experiment has been performed with a tissue mimicking phantom. The therapeutic field was applied to the phantom after 10 s from the beginning of the experiment. This lasted for 40 s and then the sample was allowed to cool down for 50 s. The collected data consists of 128 A-lines and each A-line consists of 2050 data point. Each A-line is segmented to windows with length 100, this window corresponds to 3.3 mm in phantom (Table I).

The estimated spectrum of the collected data shows three dominant peaks in the passband of the transducer. To show the frequency shifts around the heated area, we processed the data of a window around the focus point of the therapeutic field. Fig. 2

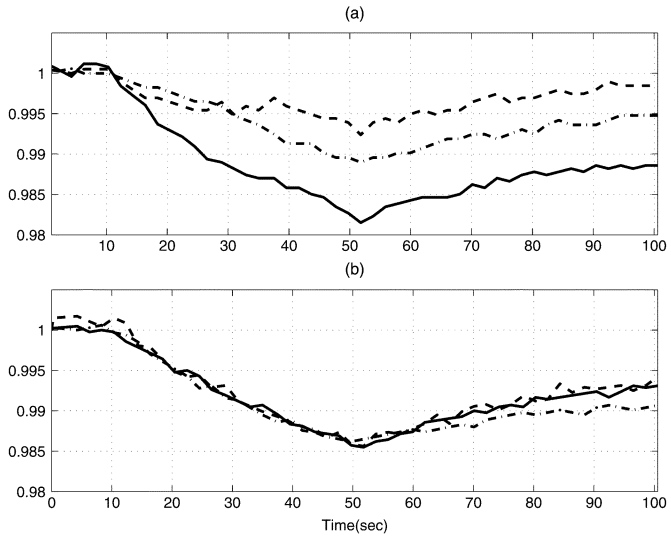

Fig. 2. Estimated frequency shift (i.e., $(f_k(t))/(f_k(0))$) (a) Classical method AR, (b) ME with IS filter.

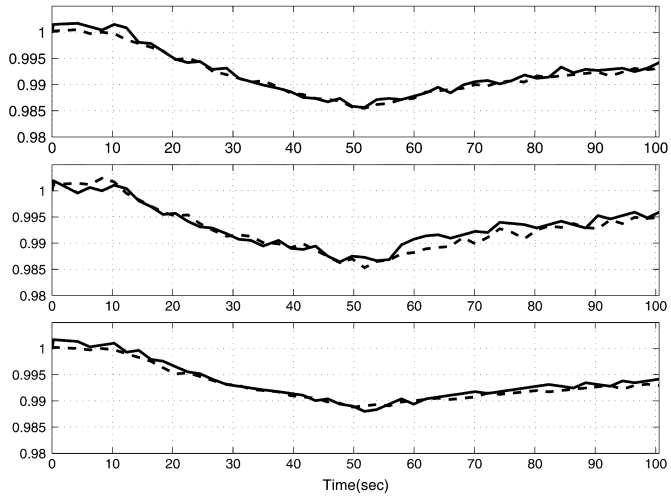

Fig. 3. Estimated frequency shift (i.e., $(f_k(t))/(f_k(0))$) in three Adjacent A-Lines via proposed algorithm.

shows the normalized resonant frequencies versus time for three harmonics. Fig. 2(a) is achieved by AR method when the order is $n = 35$. Fig. 2(b) shows the result when IS filter with $a = 0.65$ and $n = 20$ combined by ME estimator in (9) to estimate frequency shifts. It is evident that estimated frequency shifts patterns of Fig. 2(b) are quit similar and this validates the discrete scattering model. In Fig. 3, the tracked harmonics for three adjacent A-lines around the focus point have been shown (Table I).

In order to illustrate the capabilities of the presented method to estimate the temperature evolution in the medium, an experiment conducted where the therapeutic field has two focus points 4 mm apart. First we estimate the temperature at a fixed axial depth. To this end the frequency shifts were estimated by proposed algorithm and filtered by smoothing filter in Table I. In Fig. 4, a spatiotemporal (lateral-time) image of the estimated temperature has been shown. It should be noted that delivered average power to the top focus point is seventy percent of the bottom one and this explains the larger temperature change in the bottom focus point.

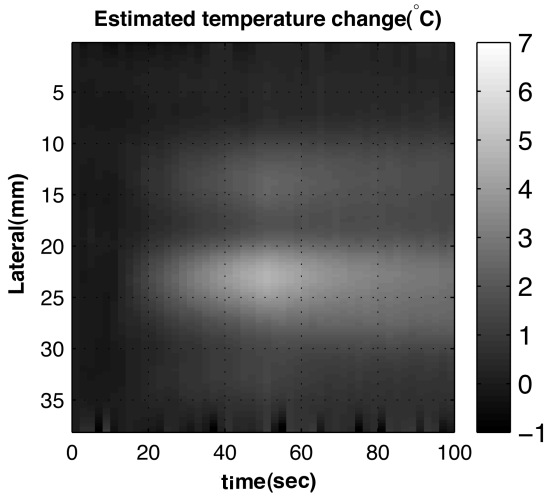

Fig. 4. Lateral temperature profile; By echo frequency shift estimation.

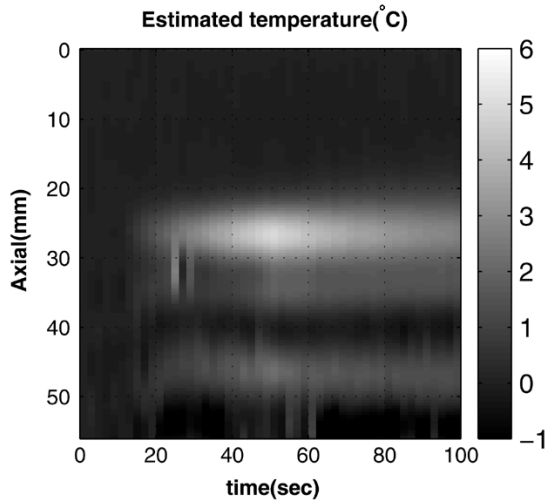

Fig. 5. Axial temperature profile; By echo frequency shift estimation.

To estimate the temperature evolution along axial direction, the A-line data is segmented to windows of length 3.3 mm and frequency shifts are estimated. Then we apply a smoothing filter as in Table I. Fig. 5 is spatiotemporal image of the estimated temperature along axial direction. The ripple observed behind the heated region in Fig. 5 is caused by thermo-acoustic lens effect which has been explained in [2]. For comparison we applied the echo time shift estimation technique explained in [2] and the resulted temperature profiles depicted in Figs. 6 and 7.

C. Bovine Muscle in Vitro Experiment

The noninvasive temperature estimation method presented in this paper can be used to provide guidance for high intensity focused ultrasound thermal therapy. In order to demonstrate this capability, an *in vitro* bovine muscle heating experiment was performed. This type of tissue present a mixture of scattering structures throughout the imaging field and require some characterization of this structure within the region being interrogated by a given data segment. For the algorithm described in this paper, this means that temperature estimation can be reliably

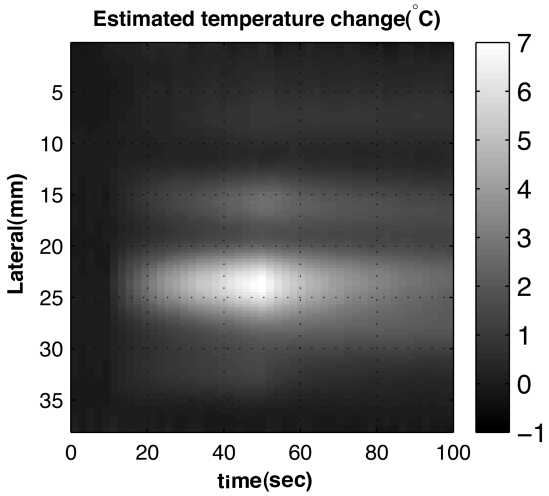

Fig. 6. Lateral temperature profile; By echo time shift estimation.

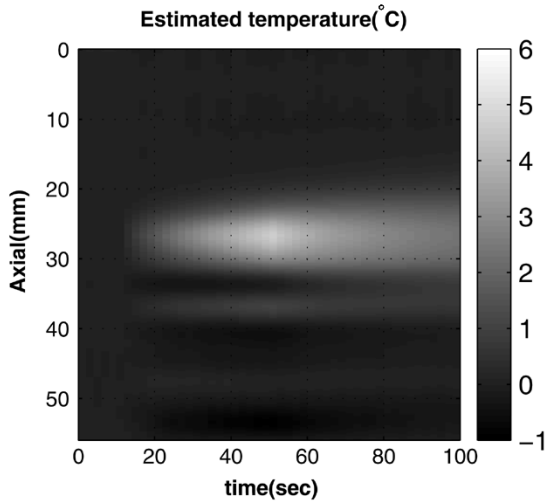

Fig. 7. Axial temperature profile; By echo time shift estimation.

performed only when the underlying regular scatterer model is valid. To identify these locations we use the fact that different harmonics should exhibit similar relative frequency shifts. The *in vitro* experiment described here illustrates this point.

The experiment was performed by the setup shown in Fig. 1, in which the phantom was replaced with an approximately parallelepiped sample of bovine muscle tissue. The heating pattern was eight 2-s single-focus patterns applied at one minute intervals at eight different locations along the y axis with a spacing of 2 mm. The therapeutic array was physically moved to produce each heating pulse moving progressively toward the imaging transducer. The frequency shifts were estimated at a point near the top of the sample, i.e., the heating points get closer to the observation point as time goes on. Fig. 8 shows frequency shifts in a location that consistent harmonics could be identified. The time evolution of the (relative) frequency shift curve is quite consistent with the turn-on and turn-off time of the therapeutic transducer. Furthermore, the increased frequency shift with the increased proximity of the heating points to the observation point is also clear from this result. It is interesting to note

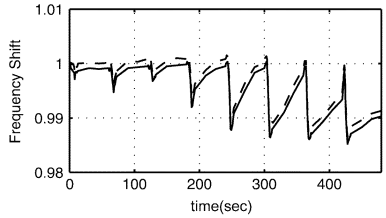

Fig. 8. Frequency shifts in bovine muscle tissue.

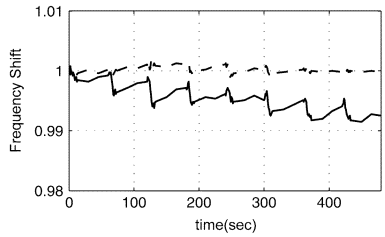

Fig. 9. Frequency shifts in bovine muscle tissue.

that the third heating pattern produced smaller temperature rise than the second one.

The scattering structure of the tissue region contributing to the echo segment affects the quality of the temperature estimate obtained by the algorithm described in this paper. The quality of the spectral estimate of the frequency shifts is related to the existence of two or more harmonics with (approximately) the same relative frequency shift. To appreciate this point, the results shown in Fig. 8 should be compared with those shown in Fig. 9. The latter was obtained from a data segment which is 1 mm from the data segment that produced Fig. 8. One can see that the relative frequency shift patterns shown in Fig. 9 are inconsistent with each other, implying the lack of dominant regular scatterers. This lack of consistency between the tracked harmonics can be used as a quality index or figure of merit of the temperature estimate obtained using this particular window. This means that we generally cannot produce contiguous estimates leading to a temperature image. Fortunately, however, most tissues have numerous locations where the regular scatterer model is valid (due to vascularization).

V. Discussion

The discrete scattering model predicts the existence of harmonics of a fundamental frequency in the backscattered ultrasound from a medium with regular scatterers. Also there is a linear relationship between the fundamental frequency change and the temperature change. We developed an algorithm based on the new spectral analysis formalism, introduced in [11], to estimate the frequency shifts in echoes from a medium undergoing heating by a therapeutic heating field. This enabled us to detect several harmonics, which has similar (identical) relative frequency shift patterns, in the echo from a tissue mimicking phantom. This observation, which was not possible with classical high resolution spectral estimation techniques [1], supports the assumptions of the theoretical model. The estimated frequency shifts were used to determine the temperature evolution in the medium.

The echo signal can be used in a different way to estimate the temperature. It was shown in [18] that there is a linear relationship between the temperature-change and echo shifts. The analysis of the estimated temperature profiles resulted from these two techniques show that both of the techniques act similarly in the heated regions. However, they both suffer from artifacts in the regions behind the heated area which is known as thermo-acoustic lens effect [2]. This provides an opportunity for compounding temperature estimates from both methods to improve the overall quality and accuracy of noninvasive temperature estimation.

An important advantage of spectral approach to temperature estimation is the potential for quantitative temperature estimation. It is possible to envision an algorithm which uses the echo-shift estimation methods described in [2] to improve the spectral estimation results and, consequently, improve the quantitative accuracy of the temperature estimation. It is important to note, however, that quantitative temperature measurements are possible when the echoes from the region under test are (largely) due to regular scatterers. That is, specular and diffuse scatterers do not produce harmonics. For these other scattering structures, other spectral models may have to be developed. Based on the model described in this paper, application of the algorithm in real tissue media with mixture of scattering structures requires some level of characterization of the scatterers. The presence of regular scatterers is fairly straightforward and there are a number of robust algorithms for the estimation of mean scatterer spacing [3], [18]. Several techniques for characterizing specular and diffuse scatters also exist (one of the better motivated approaches is described in [19]).

The *in vitro* bovine muscle experiment was meant to illustrate the limitation mentioned in the previous paragraph. The results from this suggest that only points where the existence of regular scatterers within the echo segment can produce consistent shifts in the relative frequency at more than one harmonic. This means that the proposed algorithm will produce temperature estimates at various locations on the ultrasonic image. Fortunately, many tissue organs of interest (e.g., liver and kidney) are largely homogeneous and echoes from these organs are dominated by regular scatterers. Even for more heterogeneous and/or anisotropic structures (e.g., muscle and breast), one can expect that a large number of valid temperature measurement points (or islands) can be found throughout the image.

This paper does not address some of the outstanding limitations of noninvasive temperature estimation based on pulse-echo ultrasound. One example is tissue heterogeneity, especially the presence of fatty tissue, which behaves differently from most tissue in response to temperature change. Another problem is the temperature estimation when the baseline temperature [T_0 in (3)] is a function of space. It is our view that these and other problems such as the thermal lens effect described in [2] will be solved using a two-step approach to temperature estimation. In the first step, estimation of raw temperature field can be obtained using techniques similar to the one described in this paper or in [2]. In the second step, a temperature reconstruction from noisy estimate employing physical constraints (e.g., based on the bio-heat transfer equation) can be used. This is the subject of a future report on this topic. It is important to emphasize, however, that the high-resolution technique introduced herein provides a potentially valuable means to characterize the temperature measurement at every point. Namely, the presence of two or more harmonics having the same relative frequency change as demonstrated in Figs. 3 and 8. This *figure-of-merit* characterizing the available temperature field could be the key to the success of any two-step algorithm similar to the one described in this section.

VI. Conclusion

We have presented a new algorithm for noninvasive temperature estimation based on the tracking of (relative) frequency shifts in the spectrum of an echo segment from a region undergoing temperature change. The IS high-resolution spectral estimation method was shown to produce consistent relative frequency shifts from two or more harmonics related to the mean scatterer spacing in the region. This consistency is a key improvement over previously considered high-resolution spectral estimation models (e.g., conventional ME). Temperature estimation results from tissue-mimicking phantoms have shown that the new method produces temperature estimates similar to those obtained using the echo-shift tracking technique, but with different artifacts. This suggests that the two methods are suitable for compounding to improve the overall accuracy of temperature estimation.

References

[1] R. Seip and E. Ebbini, "Noninvasive estimation of tissue temperature response to heating fields using diagnostic ultrasound," *IEEE Trans. Biomed. Eng.*, vol. 42, no. 8, pp. 828–839, Aug. 1995.

[2] C. Simon, P. VanBaren, and E. Ebbini, "Two-dimensional temperature estimation using diagnostic ultrasound," *IEEE Trans. Ultrason., Ferroelect., Freq. Contr.*, vol. 45, no. 7, pp. 1088–1099, Jul. 1998.

[3] K. Wear, R. Wagner, M. Insana, and T. Hall, "Application of autoregressive spectral analyisis to cepstral estimation of mean scatterer spacing," *IEEE Trans. Ultrason., Ferroelect., Freq. Contr.*, vol. 40, no. 1, pp. 50–58, Jan. 1993.

[4] T. T. Georgiou, "Spectral estimation via selective harmonic amplification," *IEEE Trans. Automat. Contr.*, vol. 46, no. 1, pp. 29–42, Jan. 2001.

[5] C. Byrnes, T. T. Georgiou, and A. Lindquist, "A new approach to spectral estimations tunable high-resolution spectral estimator," *IEEE Trans. Signal Process.*, vol. 48, no. 11, pp. 3189–3205, Nov. 2000.

[6] H. Nayeb-Hashemi, A. Harrison, and A. Vaziri, "Dynamic response of a heat damaged fiber-resin beam subjected to harmonic forcing at the tip," *J. Composites Technol. Res.*, vol. 25, pp. 87–95, Feb. 2003.

[7] L. Kinsler, A. Frey, A. Bahn, and J. Greenleaf, *Fundamentals of Acoustics*. New York: Wiley, 1982.

[8] L. Weng, J. M. Reid, P. M. Shankar, K. Soetanto, and X. Lu, "Application of autoregressive spectral analyisis to cepstral. Estimation of mean scatterer spacing," *IEEE Trans. Ultrason., Ferroelect., Freq. Contr.*, vol. 39, no. 5, pp. 352–358, May 1992.

[9] L. Weng, J. Reid, P. Shankar, K. Soetanto, and X. Lu, "Non-uniform phase distribution in ultrasound speckle analysis—Part II: Parametric expression and a frequency sweeping technique to measure mean scatterer spacing," *IEEE Trans. Ultrason., Ferroelect., Freq. Contr.*, vol. 39, no. 5, pp. 360–365, May 1992.

[10] P. Stoica and R. Moses, *Introduction to Spectral Analysis*. Upper Saddle River, NJ: Prentice-Hall, 1997.

[11] T. T. Georgiou, "Spectral analysis based on the state covariance: The maximum entropy spectrum and linear fractional parametization," *IEEE Trans. Automat. Contr.*, vol. 47, no. 11, pp. 1811–1823, Nov. 2002.

[12] ——, "Signal estimation via selective harmonic amplification: Music, redux," *IEEE Trans. Signal Process.*, vol. 48, no. 11, pp. 780–790, Nov. 2002.

[13] A. Nasiri Amini and T. T. Georgiou, "Statistical analysis of state-covariance subspace methods," in *Proc. IEEE Conf. Decsion and Control*, Las Vegas, NV, Dec. 2002, pp. 2633–2638.

[14] A. Nasiri Amini, "State covariance spectral estimation," M.Sc. thesis, Univ. Minnesota, Minneapolis, 2003.
[15] A. Nasiri Amini and T. T. Georgiou, "Tunable spectral estimators based on state-covaraince subspace analysis," *IEEE Trans. Signal Process.*, submitted for publication.
[16] T. Hall, M. Bilgen, M. Insana, and T. Krouskop, "Phantom materials for elastography," *IEEE Trans. Ultrason., Ferroelect., Freq. Contr.*, vol. 44, no. 11, pp. 1355–1365, Nov. 1997.
[17] K. Nightingaleand, M. Palmeri, R. Nightingale, and G. E. Trahey, "On the feasibility of remote palpation using acoustic radiation forces," *J. Acoust. Soc. Am.*, vol. 110, Jul. 2001.
[18] C. Simon, J. Shen, R. Seip, and E. Ebbini, "A robust and computationally efficient algorithm for mean scatterer spacing estimation," *IEEE Trans. Ultrason., Ferroelect., Freq. Contr.*, vol. 44, no. 7, pp. 882–894, Jul. 1997.
[19] K. Donahue, L. Huang, T. Burks, F. Forsberg, and C. Picoll, "Tissue characterization with generalized spectrum parameters," *Ultrasound Med. Biol.*, vol. 27, pp. 1505–1514, Nov. 2001.

Ali Nasiri Amini (S'01) was born in Tehran, Iran, in 1979. He received the B.Sc. degree in electrical engineering from Sharif University of Technology, Tehran, in 1999 and M.Sc. in electrical engineering from University of Minnesota, Minneapolis in 2002. He is currently working toward the Ph.D. degree in the Department of Electrical and Computer Engineering, University of Minnesota.

His research interests include statistical signal processing, adaptive radar signal processing and control theory.

Emad. S. Ebbini (S'84–M'85) received the B.Sc. degree in electrical engineering/communications from the University of Jordan, Amman, Jordan, in 1985, and the M.S. and Ph.D. degrees in electrical engineering from the University of Illinois, Urbana-Champaign, in 1990. From 1990 to 1998, he was a member of the faculty of the Electrical Engineering and Computer Science Department, University of Michigan, Ann Arbor. Since 1998, he has been with the Electrical and Computer Engineering Department, University of Minnesota, Minneapolis. His research interests are in signal and array processing with applications to biomedical ultrasonics.

Dr. Ebbini received the NSF Young Investigator Award for his work on new ultrasound phased arrays for imaging and therapy in 1993. From 1994 and 1997, he was a Member of the AdCom of the IEEE Ultrasonics, Ferroelectrics, and Frequency Control Society. In 1996, he was a Guest Editor for a special issue on therapeutic ultrasound for the IEEE TRANSACTIONS ON ULTRASONICS, FERROELECTRICS, AND FREQUENCY CONTROL. He was an Associate Editor for the same transactions from 1997 to 2002. He is a Member of the Standing Technical Program Committee for the IEEE Ultrasonics Symposium and a Member of the Board of the International Society for Therapeutic Ultrasound.

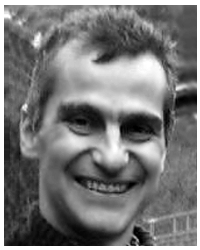

Tryphon T. Georgiou (F'00) was born in Athens, Greece, on October 18, 1956. He received the Diploma in mechanical and electrical engineering from the National Technical University of Athens, Athens, Greece, in 1979, and the Ph.D. degree from the University of Florida, Gainesville, in 1983.

He has been a member of the faculty at Florida Atlantic University (1983–1986) and Iowa State University (1986–1989). Since August 1989, he has been with the University of Minnesota where he is a Professor of Electrical and Computer Engineering. He has served as an Associate Editor for IEEE TRANSACTIONS ON AUTOMATIC CONTROL, *SIAM Journal on Control and Optimization*, and *Systems and Control Letters*, and he is currently serving on the Board of Governors of the Control Systems Society of the IEEE.

Dr. Georgiou has been a co-recipient of three George Axelby Outstanding Paper awards for the years 1992, 1999, and 2003. The first two times were for joint work with Prof. M. C. Smith (Cambridge Univ., Cambridge, U.K.), and the last time for joint work with Professors C. Byrnes (Washington Univ. St. Louis, MO) and A. Lindquist (KTH, Stockholm, Sweden).